# Effects on Oxidation Waves of Conjugated Polymers by Studying Photoluminescence Quenching and Electrogenerated Chemiluminescence

**ARTICLE** *in* THE JOURNAL OF PHYSICAL CHEMISTRY C · MAY 2011

Impact Factor: 4.77 · DOI: 10.1021/jp201577s



**6 AUTHORS**, INCLUDING:

Jiun-Tai Chen
National Chiao Tung University
**58** PUBLICATIONS **1,037** CITATIONS
SEE PROFILE

Omar Fabian
Texas A&M University
**4** PUBLICATIONS **17** CITATIONS
SEE PROFILE

Song Guo
University of Southern Mississippi
**18** PUBLICATIONS **210** CITATIONS
SEE PROFILE

THE JOURNAL OF PHYSICAL CHEMISTRY C

ARTICLE

pubs.acs.org/JPCC

# Effects on Oxidation Waves of Conjugated Polymers by Studying Photoluminescence Quenching and Electrogenerated Chemiluminescence

Jiun-Tai Chen,*[,†,‡] Ya-Lan Chang,[†] Omar Fabian,[†] Song Guo,[†] William M. Lackowski,[†] and Paul F. Barbara[†,§]

[†]Department of Chemistry and Biochemistry, Center for Nano- and Molecular Science and Technology, University of Texas at Austin, Austin, Texas 78712, United States

[‡]Department of Applied Chemistry, National Chiao Tung University, Hsinchu, Taiwan 30050

**ABSTRACT:** We study the electrochemical oxidation waves of conjugated polymers by examining photoluminescence (PL) quenching and electrogenerated chemiluminescence (ECL) of poly(9,9-dioctylfluorene-*co*-benzothiadiazole) (F8BT). Different factors such as the anion concentration, the anion size, the electrochemical potential, and the coreactant concentration are investigated for their effects on the behavior of the oxidation waves. Our results show that the wave speeds of PL quenching or ECL can be increased by increasing the anion concentration, decreasing the anion size, or increasing the electrochemical potentials. In addition, the intensity of ECL can be controlled by the coreactant concentration. The transition from pinned to free ECL waves is also studied when an intermediate coreactant concentration is used. These results provide useful insights for understanding the electrochemical oxidation wave phenomenon.

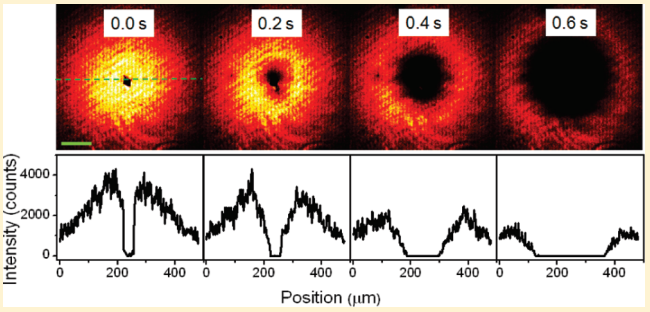


## INTRODUCTION

In recent years, conjugated polymers have aroused great interest among researchers because of their unique optical and electronic properties.[1,2] Photoluminescence (PL), electroluminescence (EL), and electrogenerated chemiluminescence (ECL) of various kinds of conjugated polymers have been studied and used for applications in different fields such as sensors or displays.[3−5] ECL is the process where electrochemically generated species undergo electron transfer reactions to form excited state molecules which decay to the ground state with emission of light.[4,6] Recently, we discovered a new phenomenon of soliton-like ECL waves from the conjugated polymer, poly(9,9-dioctylfluorene-*co*-benzothiadiazole) (F8BT).[7] ECL waves are initiated from leaks or shorts, which can be generated by scratches, defects, or gold nanoparticles (Au NPs). For example, electrical short occurs by using Au NPs which function as direct electrical connections through the film and local electrochemical double layers are formed. The soliton-like ECL wave is a special form of the oxidation wave that involves the transition from nonoxidized to oxidized states of the polymers.[7,8] At first, the polymer is not oxidized and is in a dry state. After the application of the electrochemical potential, the polymers near the scratches or shorts where double layers are formed get oxidized and holes are injected from the cathode (ITO) to the HOMO level of the polymers. In the oxidation process, the anions enter the polymer film to maintain charge neutrality, and the solvent molecules accompany the anions into the polymer film to avoid the loss of the solvation energy.[9] Solvent molecules also move into the polymer film because of the osmotic effect.[10] Consequently, the double layers move forward into the polymer films, and the oxidation wave keeps propagating. The volume of the polymer film increases due to the ingress of the anions and solvent molecules into the polymer film after the oxidation of the polymers.[11]

Although we have reported the discovery of soliton-like ECL waves, the detailed mechanism and the factors related to the initiation and propagation of the oxidation wave are still not clear. Other groups have reported moving redox fronts in conjugated polymers and proposed different models,[12−15] but they mainly focus on conjugated polymers made by electropolymerization whose electrical and mechanical properties are different from our spin-coated polymer films. In addition, the initiation of the oxidation, which is a crucial part in our study, is not emphasized in their reports. Here we study different factors such as the anion concentration, the anion size, the electrochemical potential, and the coreactant concentration on the behavior of the oxidation waves. These factors are important for understanding the mechanism and the model of the oxidation wave phenomenon, which would be crucial for applications such as novel conjugated polymer devices and artificial muscles.[16,17] We are interested in how the wave behavior including the wave speed depends on these factors. Both PL quenching and ECL, two new and unique

**Received:** February 17, 2011
**Revised:** April 22, 2011
**Published:** May 02, 2011

ways to study the transport of oxidation waves in conjugated polymers, are used in this work. When the polymers are oxidized, the PL is quenched by the injected holes, and oxidation waves can be observed in the form of PL quenching waves. It has been shown that for the case of a single F8BT molecule the efficiency of PL quenching is approaching 100% for injection of a single positive charge.[18] Ag and Au nanoparticles can also exhibit extraordinary PL quenching effects on conjugated polymers.[19] ECL is another way to study the oxidation wave in conjugated polymer films, and the process involves the oxidation of polymers and the electrochemical reaction with the coreactants.[7,8] We propose that the ECL waves are emitted from the top of the polymer films. The main results in this paper show that the behavior of oxidation waves in F8BT films is strongly affected by different experimental factors such as the anion concentration, the anion size, the electrochemical potential, and the coreactant concentration. The wave speed, for example, can be increased by increasing the anion concentration, decreasing the anion size, or increasing the electrochemical potential. Furthermore, the intensity of the ECL waves can be enhanced by increasing the concentration of the coreactant, tripropylamine (TPA). The results from PL quenching wave show more linear behavior than the results from ECL because the coreactant, TPA, is not involved in the PL quenching experiments. With intermediate concentration of TPA, the transition from pinned to free ECL waves is also studied. The pinned ECL wave is assumed to first generate on the top part of the polymer film and then sink down to reach the ITO substrate for the ECL wave to propagate.

## EXPERIMENTAL SECTION

**Materials.** Poly(9,9-dioctylfluorene-*co*-benzothiadiazole) (F8BT ($M_w$: 60, 70, and 140 kg/mol) were obtained from American Dye Source. Tri-*n*-propylamine (TPA) and acetonitrile (MeCN) were obtained from Acros. Lithium perchlorate ($LiClO_4$) and lithium trifluoromethanesulfonate ($LiCF_3SO_3$) were purchased from Sigma-Aldrich. Silver wires (25 $\mu$m in diameter) are obtained from Goodfellow. ITO substrates were purchased from Metavac. F8BT films with thickness of 50 and 250 nm were made by spin-coating 150 $\mu$L of F8BT solutions (14 and 28 mg/mL in toluene) onto cleaned ITO substrates at 2000 rpm for 60 s, respectively. The thickness of the polymer films was measured by atomic force microscopy (AFM) as follows: The polymer film was first scratched by a near-field scanning optical microscopy tip (size ~50 $\mu$m). Then the thickness of the polymer film was extracted from the cross sections of the AFM scans across the scratch. The spin-coated film can be controlled by the spin speed, and the roughness is less than 5 nm.

**Cell Fabrication.** The configuration and fabrication process of the electrochemical cells are described elsewhere in more detail.[18] The scratches on the polymer films were made by an NSOM tip. The MeCN solution contains electrolyte ($LiClO_4$ or $LiCF_3SO_3$) and the coreactant, tripropylamine (TPA), for the ECL experiment. A wide-field microscope (Nikon, Eclipse TE2000) and a CCD camera (Roper Scientific, Cascade 512B) are used to obtain the PL and ECL images. A potentiostat (Autolab, PGSTAT 100) is used to provide the electrochemical potentials related to QRE (Quasi reference electrode). The electrochemical potentials are 0.20 ± 0.04 V more negative than those for QRE for the ferrocenium/ferrocene ($Fc/Fc^+$) couple internal standard.

## RESULTS AND DISCUSSION

We study different effects on the behavior of the oxidation waves of spin-coated F8BT films by examining the PL quenching and the ECL waves. F8BT is a commonly used material for applications such as organic light-emitting diode (OLED) or light-emitting electrochemical cells (LEC).[20,21] For the PL quenching and ECL experiments in this study, the waves are launched from leaks which are made by intentional scratches.[7] These scratches (~50−100 $\mu$m in size) are made by a near-field optical microscopy (NSOM) tip. When a polymer film is prepared without scratches, no electrochemical oxidation wave is observed unless some defects are present in the polymer film. By making intentional scratches, the ITO substrate at the scratched region is exposed to the electrolyte solution before the application of the electrochemical potential. After the electrochemical potential is applied, electrochemical double layers are formed at the interface between electrolyte solution and the ITO substrate. Therefore, electrochemical reaction of the polymer film starts from the three-phase regions including the electrochemical double layer, the polymer film, and the electrolyte solution.[7,8] Consequently, the oxidation waves are launched from these regions and propagate laterally throughout the polymer films. Without scratches, electrolyte solution could not reach the ITO substrate and no electrochemical double layer is formed, resulting in no electrochemical oxidation of the polymer film. The effects of scratches can also be observed in the case of using very thin polymer film with the thickness of 15 nm.[8] When the polymer film is as thin as 15 nm, dendritic ECL filaments are observed after applying the electrochemical potential as a result of drying cracks that serve similar functions as scratches. The drying cracks are exposed to the electrolyte solution, and the electrochemical double layers are formed in these regions when the electrochemical potential is applied, resulting in the simultaneous oxidation of polymers.

**Anion Concentration and Anion Size.** During the oxidation process, anions diffuse into the polymer films to compensate the positive charges for maintaining charge neutrality.[9] We would like to know if anions are the limiting factors for the oxidation process. The rate of oxidation might be limited by the anion concentration or the anion size even when an oxidation overpotential is established.[22] We first study the anion concentration effect on the behavior of the PL quenching wave of F8BT films. The polymer films are excited by an Ar ion laser at wavelength of 488 nm in the PL quenching experiments. Figure 1 shows the PL images of the F8BT film at different time sequences after the application of the electrochemical potential at 1.5 V with 0.02 M $LiClO_4$. The electrochemical potential at 1.5 V is chosen here because this value is higher than the half-wave oxidation potential ($E_{1/2}$) of F8BT (~1.2 V), which allows an overpotential to be established and polymer chains can be oxidized. Higher electrochemical potential can result in higher electrochemical oxidation speed, which will be discussed later in this paper. The electrochemical potential at 1.5 V is a suitable condition for studying the effect of anions concerning that higher oxidation speed is difficult to be observed using the microscope. Different colors in the figures represent different intensities of the fluorescence. The upper left image in Figure 1 shows the PL before applying the electrochemical potential. The black region in the center of the graph is the region that is scratched by the NSOM tip, in which no or very little polymers are present. After the application of the electrochemical potential, an overpotential is established and the

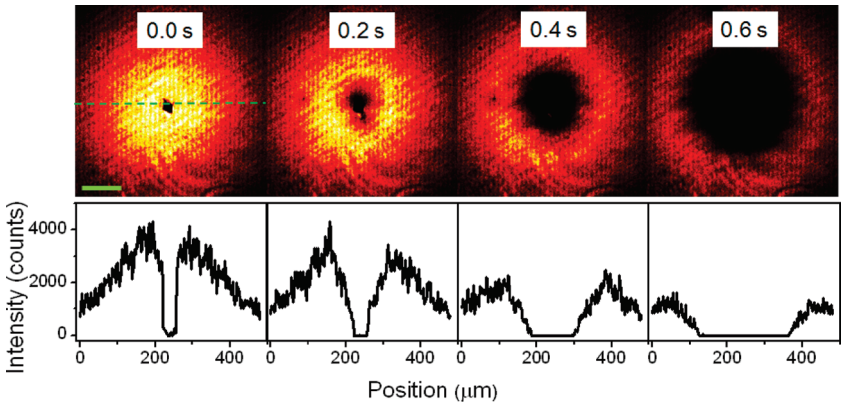


**Figure 1.** Images of PL quenching of F8BT films ($M_w$ = 60 kg/mol, film thickness ~50 nm) on the ITO substrates in the MeCN solution of 0.02 M $LiClO_4$. The scale bar is 100 $\mu$m, and the integration time of all images is 100 ms. The top panel shows the PL images at 0.0, 0.2, 0.4, and 0.6 s after the application of 1.5 V. The bottom panel shows the line scans for the corresponding PL images. The speed of the quenching wave is ~200 $\mu$m/s by considering the positions at 50% quenching.

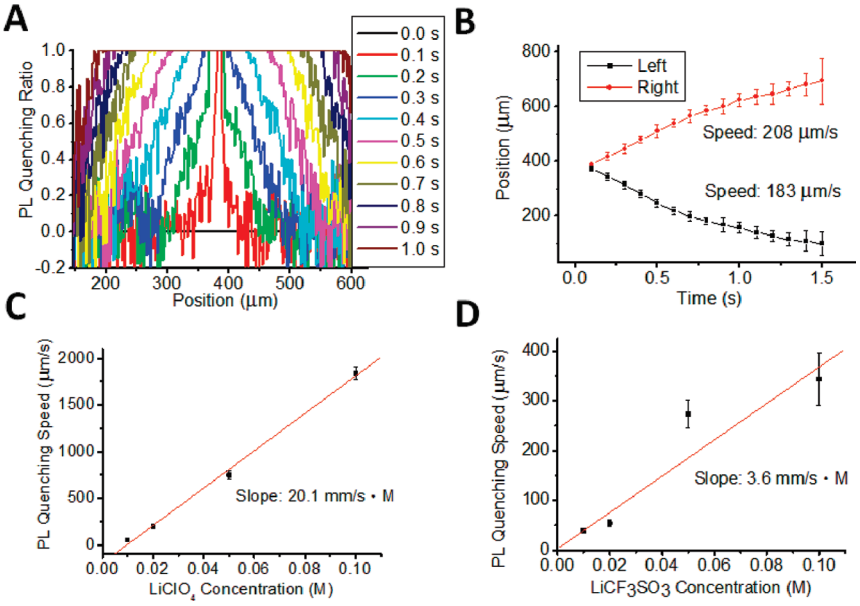


**Figure 2.** PL quenching of F8BT films ($M_w$ = 60 kg/mol, film thickness ~50 nm) on the ITO substrates in the MeCN solution after the application of 1.5 V. (A) Plot of the PL quenching ratio versus the position for the sample using 0.02 M $LiClO_4$. (B) Plot of the position at 50% PL quenching versus time for the samples using 0.02 M $LiClO_4$. The black and red lines show the line scans from the left and right side of the scratch, respectively. (C) Plot of the PL quenching speed versus the $LiClO_4$ concentration. The slope is 20.1 mm/(s M), and the intercept is −195.3 $\mu$m/s. (D) Plot of the PL quenching speed versus the $LiCF_3SO_3$ concentration. The slope is 3.6 mm/(s M), and the intercept is 16.8 $\mu$m/s.

double layer is formed in the scratched region. Oxidation starts from the polymers near the double layers and the oxidative waves are initiated.[7] Except the scratched region, the PL in Figure 1 is stronger in the center and weaker at the edge before the application of the electrochemical potential, which is due to the nonuniform intensity of the Ar ion laser (488 nm). When the electrochemical potential is held at 0 V, PL does not change appreciably, showing the stable emission from F8BT polymers. After applying the electrochemical potential at 1.5 V, the polymer near the scratched region starts to get oxidized and the local PL is quenched by the injected holes. The PL quenching waves are initiated from the scratched region where oxidation of polymers starts and moves outward. Even though the shape of the initial scratch is not circular, the wave tends to form a more circular shape when the electrochemical potential is applied for longer time. The bottom panel in Figure 1 shows the line scans of the intensity versus the position. The region for the line scan is indicated as the green dashed line. The quenching region is shown to move outward starting from the scratched region.

We use the "PL quenching ratio" to determine the extent of PL quenching which is related to the degree of oxidation. The intensity at time 0.0 s is used as the basis to calculate the PL quenching ratio. The PL quenching ratio at different locations is defined by the following equation

$$\text{PL quenching ratio} = (I_0 - I_t)/I_0 \qquad (1)$$

where $I_t$ is the PL intensity after the application of the electrochemical potential for time $t$ and $I_0$ is the PL intensity before the electrochemical potential is applied. The position at which the

PL intensity is quenched 50% is used to calculate the speed of the PL quenching wave. In our previous studies of F8BT single molecules, the electrochemical potential where the PL is quenched by 50% was also used as an indirect way to determine the electrochemical half-wave potentials.[18]

Figure 2A shows the PL quenching ratio versus the position after the application of 1.5 V at different time sequences for the sample using 0.02 M $LiClO_4$. The PL quenching ratio is calculated by eq 1 using the data from the line scans in Figure 1. Higher magnitude of fluctuation is observed for the PL quenching ratio in the region away from the scratched region because of the lower initial intensity. The positions at 50% PL quenching are used to calculate the speed of the PL quenching wave. Figure 2B shows that the positions at 50% PL quenching change with time. The black and red curves represent the data from the line scans on the left and right sides of the scratch, respectively. The nonlinearity in the plot of position versus time is probably attributed to the *IR* drop of the polymer film away from the scratched region. *IR* drop means voltage drop across the polymer film, and $I$ and $R$ stand for current ($I$) and resistance ($R$), respectively. The effect from the *IR* drop is more obvious if we use a top Au electrode on the polymer film instead of using the underlying ITO substrate. In the case of the top Au electrode, the waves finally stop due to the *IR* drop. The nonlinearity might also be due to the rough interface between the polymer film and the electrolyte solution which is created by the scratching process. The larger interfacial area of the rough interface might result in more available anions for compensating the oxidized polymers. This issue could be resolved by using other ways of initiating the electrochemical oxidation waves or by creating smaller scratches.

Despite the nonlinearity in the curves of the position versus time, the line scans on the left and right sides of the scratch are fitted with a linear function for the convenience of studying the effect of anion concentrations. The speeds are fitted to be 183 and 208 $\mu$m/s for the line scans on the left and right sides of the scratch, respectively. Similar data processing is performed, and the speeds of PL quenching for different $LiClO_4$ concentrations are obtained, as shown in Figure 2C. The speed is shown to increase with the $LiClO_4$ concentration, and the slope is 20.1 mm/(s M) when the data are fitted to a linear function. For the PL quenching experiment, the polymer is ready to get oxidized once a high enough electrochemical potential is applied, and an overpotential is established. But the speed of oxidation is also affected by the transport of anions which are responsible for maintaining charge neutrality. There are three mechanisms for the anion transport including convection, diffusion, and migration.[23] Convection is the movement of a particle carried in the flow of a fluid and is not considered here because there is no significant fluid flow through the polymer film during the electrochemical oxidation process.[24] For the diffusion mechanism, it has been pointed out that the diffusion of ions in conjugated polymer films is not Fickian considering the chain movement, the degree of polymer solvation, and ion−polymer interaction.[12,25] Therefore, the diffusion coefficient of the flux of ions is also a function of ion concentration and could not be obtained using the Stokes−Einstein equation. Migration is the third possible mechanism that the ions move under local electric fields. Lacroix et al. have done a theoretical analysis of mass transport in the switching of conductive polymers to show the ion transport could be described as a migration phenomenon, rather than a diffusion phenomenon.[14] When the ion transport is dominated by migration, Smela et al. have shown that the speed

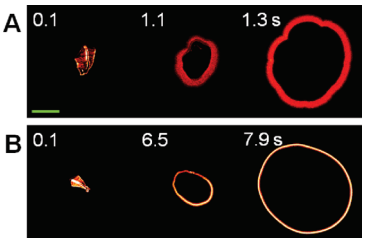


**Figure 3.** ECL images from F8BT films ($M_w$: 70 kg/mol, film thickness ~250 nm) on the ITO substrates in the MeCN solution of 0.1 M TPA and 0.1 M of electrolytes, $LiClO_4$ (A) and $LiCF_3SO_3$ (B). The time after the application of 1.8 V pulsed bias is labeled on the left top corner of each image. A scratch was made by an NSOM tip on the film. The scale bar is 200 $\mu$m, and the integration time of each image is 100 ms.

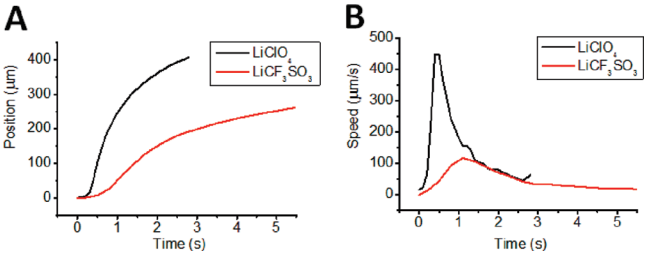


**Figure 4.** ECL data from F8BT films ($M_w$: 70 kg/mol, film thickness ~250 nm) on the ITO substrates in the MeCN solution of 0.1 M TPA and 0.1 M supporting electrolytes of $LiClO_4$ (black curve) and $LiCF_3SO_3$ (red curve). A scratch was made by an NSOM tip on the film. A potential step from 0 to 1.8 V is applied at 0 s. (A) Plot of the position at maximum ECL versus time. The positions are obtained at maximum ECL intensities in the line scans. (B) Plot of the wave speed versus time.

of the moving front is proportional to the electrochemical potential. But our results demonstrate that the speed of the oxidation wave is more exponentially dependent rather than linearly proportional to the electrochemical potential. Therefore, the dominant mechanism of the anion transport in our study is assumed to be non-Fickian diffusion.

Instead of the perchlorate ion ($ClO_4^-$) from lithium perchlorate ($LiClO_4$), we also use another anion, trifluoromethanesulfonate ($CF_3SO_3^-$), from lithium trifluoromethanesulfonate ($LiCF_3SO_3$) in the PL quenching experiments to study the anion size effect on the behavior of the PL quenching and ECL waves. The ion volume of $CF_3SO_3^-$ (86.9 Å$^3$) is larger than the ion volume of $ClO_4^-$ (54.4 Å$^3$).[26] Figure 2D shows the PL quenching speed versus the $LiCF_3SO_3$ concentration. Similar to the case of $LiClO_4$, constant PL quenching speeds are observed. The speed increases with the $LiCF_3SO_3$ concentration, and the slope is 3.6 mm/(s M). But the speed of the PL quenching wave for $LiCF_3SO_3$ is slower than the speed for $LiClO_4$ when the same concentration is used. For example, the speed of the PL quenching wave is ~400 $\mu$m/s for $LiCF_3SO_3$ while the speed is ~1800 $\mu$m/s for $LiClO_4$ when the anion concentrations are 0.1 M. Assuming that diffusion depends on free volume, Yasuda et al. have shown that the size of the diffusant strongly affects the diffusion coefficient in the case of non-Fickian diffusion by studying permeability of solutes through hydrated polymer membranes.[27] They have demonstrated that there is an inverse exponential relationship between the size of the diffusant and the diffusion coefficient.[28] In our case here, the size of the anion

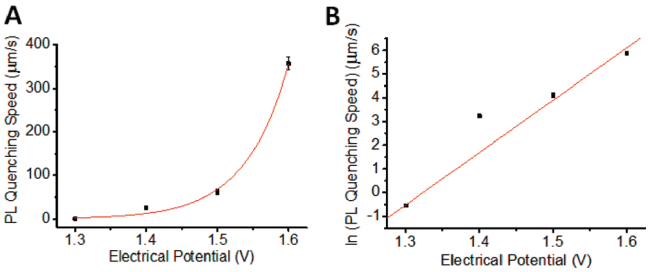


**Figure 5.** PL quenching of F8BT films ($M_w$ = 60 kg/mol, film thickness ~50 nm) on the ITO substrates in the MeCN solution of 0.01 M $LiClO_4$. (A) Plot of the speed of the PL quenching waves versus the electrochemical potential. (B) Plot of the natural log of the speed of the PL quenching waves versus the electrochemical potential.

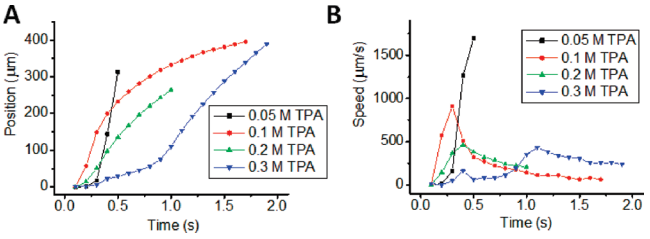


**Figure 6.** ECL waves of F8BT films ($M_w$ = 60 kg/mol, film thickness ~250 nm) on the ITO substrates in the MeCN solution of 0.01 M $LiClO_4$. Electrochemical potentials step from 0 to 1.8 V are applied at 0 s. (A) Plot of the position at maximum ECL versus time for different TPA concentrations. (B) Plot of the speed of the ECL wave versus time for different TPA concentrations.

$CF_3SO_3^-$ is 1.6 times bigger than the size of the anion $ClO_4^-$ and is expected to have a 5 times smaller diffusion coefficient when the inverse exponential relationship is considered. Note that the actual size of diffusant need to be considered might be the size of the ion clusters including the holes, anions, and solvent molecules which diffuse together when the oxidation waves are transporting.

For different anion sizes ($ClO_4^-$ and $CF_3SO_3^-$), we also try the experiments of ECL waves by adding the coreactant (TPA) into the solution and applying the electrochemical potential. In the ECL experiments, the laser is not used and therefore PL is not observed. Figure 3 shows the ECL images from the F8BT film for $LiClO_4$ (A) and $LiCF_3SO_3$ (B). Similar to the PL quenching waves, the ECL waves are launched from the scratched region. The speed of the ECL wave for $ClO_4^-$ is faster than the speed for $LiCF_3SO_3$. At time 1.3 s, the ECL wave for $ClO_4^-$ has already traveled for ~200 $\mu$m while it takes longer time (7.9 s) to travel similar distance when $CF_3SO_3^-$ is used as the anion. The width of the wave is also broader when $ClO_4^-$ is used as the anion because of the faster speed of the waves. The broadening in width of the ECL wave is related to the integration time we use (100 ms) and is referred to as the "time blurring", which is proportional to the wave speed.

Figure 4A shows the positions at maximum ECL versus time for $LiClO_4$ and $LiCF_3SO_3$. Different from the PL quenching results shown in Figure 2B, the curve for the ECL wave is not linear and the speed is not constant at different time sequences. This nonlinear behavior of the ECL wave is due to the use of the coreactant, TPA, which is not present in the PL quenching experiments. In the ECL process, the oxidized F8BT polymers are reduced by TPA radicals and the oxidation speeds are decreased.[29] Other effects of TPA on the behavior of oxidation waves will also be discussed later in this paper. Figure 4B shows the plot of the wave speed versus time for $LiClO_4$ and $LiCF_3SO_3$ based on the data in Figure 4A. Both curves show that the speeds increase to maximum speeds and then decrease. For $LiClO_4$, the wave reaches a maximum speed of 450 $\mu$m/s at ~0.5 s. For $LiCF_3SO_3$, the wave reaches a maximum speed of 120 $\mu$m/s at 1.2 s. The results from the ECL waves also support our previous conclusion that the penetration of charge-compensating anions into the F8BT film is essential for oxidation reaction, and it is harder for larger anions to penetrate into the film than smaller anions.

For the extent of swelling by the solvent molecules and anions, we have conducted AFM measurements in our previous study.[7] For a 250 nm F8BT film, the actual swelling at the time the ECL wave passes the tip (i.e., < 0.1 s) is below our resolution (2 nm). This indicates that very little solvent and anions are in the swollen polymer film. When the electrical potential is held at +1.7 V for an extended period (>60 s), the film will ultimately buckle and delaminate, due presumably to the stress in the film created by the EC-induced swelling.

**Electrochemical Potential.** We also study how the behavior of the oxidation wave depends on the electrochemical potential. If the applied electrochemical potential is lower than the half-wave oxidation potential ($E_{1/2}$), polymers are not oxidized and no wave is formed. When the electrochemical potential is higher than the $E_{1/2}$ of F8BT (~1.2 V), an overpotential is established and polymer starts to get oxidized.[29] Note that there will be more irreversible degradation of the F8BT polymers when the electrochemical potential is higher. This irreversible electrochemical reactions of F8BT is also discussed previously for F8BT nanoparticles.[30]

We study the effect of the electrochemical potential by examining the PL quenching waves. Figure 5A shows that the speed of the PL quenching wave increases with time and is fitted with an exponential function. Figure 5B shows the natural log of the speed of the PL quenching waves versus the electrochemical potential. The exponential relationship between the speed of oxidation and the electrochemical potential is also observed by Otero et al. for studying the oxidation of polypyrrole or polyaniline.[9,25] They have proposed a electrochemically stimulated conformational relaxation model that the conformational relaxation time, the time required to change the conformation of a polymeric segment, can be reduced by increasing the electrochemical potential. Our results show similar behavior and the speed of the oxidation wave increases with the electrochemical potential. Another thing to note is that the F8BT thin film can be quenched by the electric field effect.[31] We not that the electric field effect from the ITO substrate on the PL quenching might occur independently on the whole film. Since the speeds are calculated based on the relative PL quenching ratios, the electric field effect from the ITO substrate is expected to affect only the PL quenching values, but not the speeds of the oxidation waves.

**Coreactant Concentration.** Tripropylamine (TPA) is used as the coreactant in the electrochemical reaction for producing ECL.[29] After oxidation followed by deprotonation, a strong reducing intermediate (TPA radical) is formed and then undergoes an electron-transfer reaction with the oxidized polymer to generate light.[29,32] The electron is transferred from the HOMO level of the TPA radical to the LUMO level of the oxidized polymer, and light is generated when the molecule on the excited

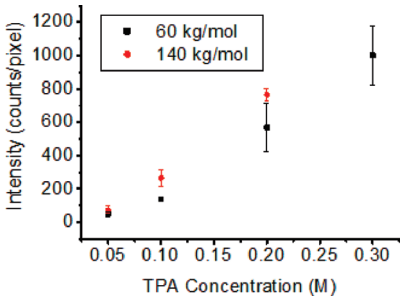


**Figure 7.** Plot of the ECL intensity versus TPA concentration of F8BT films (film thickness ~250 nm) on the ITO substrates in the MeCN solution of 0.01 M $LiClO_4$. The red and black dots show the data from F8BT with molecular weight of 140 and 60 kg/mol, respectively. The intensities are determined by averaging the intensities at each pixel of the ECL images after the application of 1.8 V.

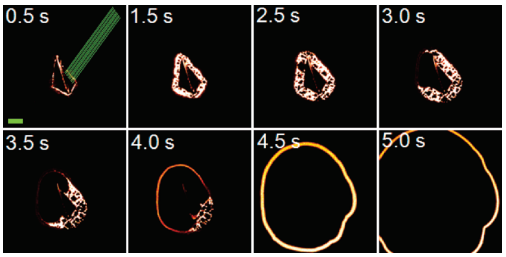


**Figure 8.** ECL images of an F8BT film ($M_w$ = 141 kg/mol, thickness ~250 nm) on the ITO substrate in the MeCN solution of 0.1 M $LiClO_4$ and 0.2 M TPA after the application of 1.8 V. The scale bar is 100 $\mu$m, and the integration time of all images is 100 ms. ECL is initiated from the scratch made by the NSOM tip. Transition from pinned to free ECL waves is observed. The data shown in Figure 9A,B are obtained from the 10 line scans indicated as the green lines in the top left image.

state decays to the ground state.[33] Therefore, when there are more TPA molecules, more ECL can be produced because more oxidized polymers are reduced back by the TPA radicals.[34] The "net" rate of the oxidation of the polymer is decreased when more TPA molecules are present. Figure 6A shows the plot of the position at maximum ECL versus time for ECL waves of F8BT for different TPA concentrations. The positions are obtained at maximum ECL intensities in the line scans of ECL images. Figure 6B is the plot of the speed of the ECL wave versus time, and the maximum speed is shown to decrease when more TPA molecules are added. When a lower concentration of TPA is used (0.05 M), the oxidation of the polymer is just slightly affected by the use of TPA and the speed goes up very quickly (1500 $\mu$m/s in 0.5 s). As the TPA concentration increases, the rate of polymer oxidation is further decreased. For 0.1 and 0.2 M TPA, the maximum speeds go to 900 and 500 $\mu$m/s, respectively.

The ECL intensity is also affected by the TPA concentration. Figure 7 is the plot of the average ECL intensity versus TPA concentrations for F8BT with two different molecular weights (60 and 140 kg/mol). Similar behavior is observed for the two molecular weights, and the ECL intensity increases with the TPA concentrations. With higher concentration of TPA, more TPA radicals are generated and reduce more oxidized polymers, resulting in stronger ECL.

**Transition from Pinned to Free ECL Waves.** In the last part, we have discussed the coreactant effect on the oxidation waves that TPA will reduce the speed of the oxidation waves. At some intermediate TPA concentration (0.2 −0.3 M), the transition from pinned to free ECL waves can be observed. Pinned waves are referred as the waves that stall or move at a slower speed and free waves are the ECL that propagates at a higher speed.[7] Figure 8 shows the ECL images during the transition when 0.2 M TPA is used. When the polymer is first oxidized near the scratch after the application of the electrochemical potential, a pinned wave is formed near the scratched region (0.1−1.5 s in Figure 8). Images at 2.5−4.0 s show the transition from pinned to free waves that some regions overcome the energy barrier for forming free waves. After longer time ($t$ > 4 s), the free ECL wave is formed and propagates outward. We propose that this transition is related to the pinned surface oxidation wave that sinks down to reach the bottom ITO for the free waves to propagate. Such transition is easier to be observed when an intermediate TPA concentration is used. With lower concentration of TPA (<0.2 M), the time for pinned wave is shorter and most observed ECL waves are free waves. With higher concentration of TPA (>0.2 M), the pinned wave period is longer and the transition from pinned to free ECL waves can be observed. When the TPA is too high (>0.3 M), we only observe pinned waves because of the strong reducing ability of TPA radicals. For PL quenching experiments, only free waves are observed since there is no TPA involved.

Figure 9 is the data analysis for the ECL images during the transition from pinned to free waves shown in Figure 8. Parts A and B of Figure 9 are from the line scans shown in the top left image in Figure 8. Figure 9A shows the mean maximum intensity versus time. The mean maximum intensity is stronger (~15 000 counts) during the period of pinned waves (1−3 s) and becomes weaker (~1000 counts) for free waves ($t$ > 4 s). During the period of the pinned wave, ECL is mainly generated near the scratches. More TPA molecules are supplied near the scratched regions because the oxidation wave stalls or moves in a slower speed, resulting in stronger ECL. Then the pinned surface wave sinks down to touch the ITO substrate for the free wave to form and propagate. During the period of the free wave, the ECL is generated from the top part of the polymer film even though the whole film is oxidized. This is because the TPA radical can only reach the top part of the polymer film, resulting in weaker ECL. Figure 9B shows the plot of the mean position at maximum intensity versus time. The transition from pinned to free waves can be seen at ~4 s where the wave speed suddenly increases. During the period of the pinned wave ($t$ < 4 s, the position at maximum intensity increases slower (speed ~14 $\mu$m/s). In comparison, the position at maximum intensity increases much faster (speed ~205 $\mu$m/s) during the period of the free wave ($t$ > 4 s). Instead of using the data from the line scans, we also do the analysis by integrating ECL from the whole region. Figure 9C is the integrated ECL intensity versus time. Similar to the mean maximum intensity shown in Figure 9A, the integrated ECL intensity is stronger during the period of the pinned wave than the intensity during the period of the free wave. After 4.5 s, the integrated ECL intensity is decreased because some ECL waves already transport out of the observed region, and the intensities are not completely integrated. Figure 9D shows the plot of the current versus time. Lower current ($I = 1 \times 10^{-5}$ A) are observed during the period of the pinned wave ($t$ < 4 s), showing that less polymers are oxidized. Higher current ($I = 5 \times 10^{-5}$−$3 \times 10^{-4}$ A) is observed during the period of the free wave because the whole film is oxidized even when ECL is only produced from the top

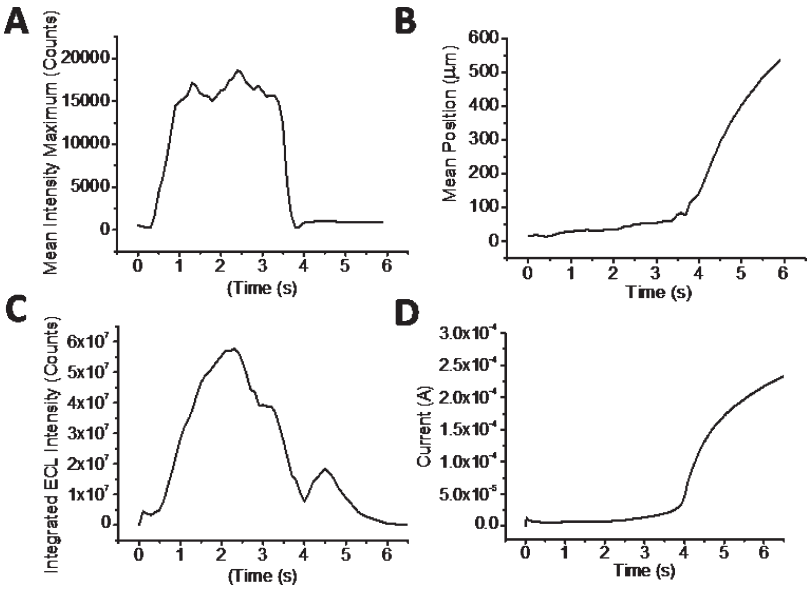


**Figure 9.** Data of the transition from pinned to free ECL waves of an F8BT film ($M_w$ = 141 kg/mol, thickness ~250 nm) on the ITO substrate with 0.2 M TPA after applying 1.8 V. Data in (A) and (B) are obtained from the line scans indicated in the top left image in Figure 8. (A) Plot of the mean intensity maximum versus time. (B) Plot of the mean position at intensity maximum versus time. (C) Plot of the integrated ECL intensity versus time. (D) Plot of the current versus time.

layer of the polymer film. It is interesting to see that the higher current occurs during the period with weaker ECL. This confirms our hypothesis that during the free waves ECL only generated from the top part of the film, while the whole film is oxidized and exhibits higher current.

## CONCLUSION

To further investigate our newly discovered soliton-like oxidation waves, we have developed PL quenching and ECL as two new and unique ways for studying the oxidation of conjugated polymers. The electrochemical oxidation behavior of spin-coated F8BT films are studied by using different experimental factors including anion concentration, anion size, electrochemical potential, and coreactant concentration. The kinetics of the wave behavior is strongly affected by these factors, and the speed or the photoluminescence intensity can be controlled. In this work, we also demonstrate the importance of using scratches, which is critical for the formation of oxidation waves that are initiated from the three-phase regions including the electrochemical double layer, the polymer film, and the electrolyte solution. The transport of anion is assumed to be dominated by non-Fickian diffusion, and the diffusion coefficient can be increased by using larger anions. Since the coreactant, TPA, is not used in the PL quenching experiments, the results from PL quenching waves show more linear behavior than the results from ECL waves. The transition from pinned to free waves is also studied. After the pinned ECL surface wave sinks and touches the electrode, more currents are generated during the free wave period, which is mainly contributed from the oxidation of the whole polymer film. The results of this paper offer useful insights for understanding the electrochemical oxidation wave phenomenon of spin-coated conjugated polymer films. Future work will include controlling the film properties by thermal and solvent annealing, which may significantly affect the polymer chain packing of the spin-coated film. In addition, other ways than scratching will be developed with an intent to avoid the creation of the rough surface at the scratched region.

## AUTHOR INFORMATION

### Corresponding Author

*E-mail: jtchen@mail.nctu.edu.tw.

### Notes

[§]Professor Paul F. Barbara passed away on October 31, 2010.

## ACKNOWLEDGMENT

This work was supported by the National Science Foundation, the Welch Foundation, and the National Science Council of Taiwan.

## REFERENCES

(1) Schwartz, B. J. *Annu. Rev. Phys. Chem.* **2003**, *54*, 141–172.
(2) Hide, F.; DiazGarcia, M. A.; Schwartz, B. J.; Heeger, A. J. *Acc. Chem. Res.* **1997**, *30* (10), 430–436.
(3) Friend, R. H.; Gymer, R. W.; Holmes, A. B.; Burroughes, J. H.; Marks, R. N.; Taliani, C.; Bradley, D. D. C.; Dos Santos, D. A.; Bredas, J. L.; Logdlund, M.; Salaneck, W. R. *Nature* **1999**, *397* (6715), 121–128.
(4) Forster, R. J.; Bertoncello, P.; Keyes, T. E. *Annu. Rev. Anal. Chem.* **2009**, *2*, 359–385.
(5) Marder, S. R.; Kippelen, B.; Jen, A. K. Y.; Peyghambarian, N. *Nature* **1997**, *388* (6645), 845–851.
(6) Miao, W. J. *Chem. Rev.* **2008**, *108* (7), 2506–2553.
(7) Chang, Y. L.; Palacios, R. E.; Chen, J. T.; Stevenson, K. J.; Guo, S.; Lackowski, W. M.; Barbara, P. F. *J. Am. Chem. Soc.* **2009**, *131* (40), 14166–14167.
(8) Chen, J. T.; Chang, Y. L.; Guo, S.; Fabian, O.; Lackowski, W. M.; Barbara, P. F. *Macromol. Rapid Commun.* **2011**, *32* (7), 598–603.
(9) Otero, T. F.; Grande, H. J.; Rodriguez, J. *J. Phys. Chem. B* **1997**, *101* (19), 3688–3697.

(10) Bay, L.; Jacobsen, T.; Skaarup, S.; West, K. *J. Phys. Chem. B* **2001**, *105* (36), 8492–8497.
(11) Suarez, M. F.; Compton, R. G. *J. Electroanal. Chem.* **1999**, *462* (2), 211–221.
(12) Wang, X. Z.; Shapiro, B.; Smela, E. *Adv. Mater.* **2004**, *16* (18), 1605–1609.
(13) Tezuka, Y.; Ohyama, S.; Ishii, T.; Aoki, K. *Bull. Chem. Soc. Jpn.* **1991**, *64* (7), 2045–2051.
(14) Lacroix, J. C.; Fraoua, K.; Lacaze, P. C. *J. Electroanal. Chem.* **1998**, *444* (1), 83–93.
(15) Otero, T. F.; Grande, H.; Rodriguez, J. *J. Electroanal. Chem.* **1995**, *394* (1−2), 211–216.
(16) Baughman, R. H. *Synth. Met.* **1996**, *78* (3), 339–353.
(17) Kaneto, K.; Kaneko, M.; Min, Y.; Macdiarmid, A. G. *Synth. Met.* **1995**, *71* (1−3), 2211–2212.
(18) Palacios, R. E.; Fan, F. R. F.; Bard, A. J.; Barbara, P. F. *J. Am. Chem. Soc.* **2006**, *128* (28), 9028–9029.
(19) Guan, Z. P.; Polavarapu, L.; Xu, Q. H. *Langmuir* **2010**, *26* (23), 18020–18023.
(20) Donley, C. L.; Zaumseil, J.; Andreasen, J. W.; Nielsen, M. M.; Sirringhaus, H.; Friend, R. H.; Kim, J. S. *J. Am. Chem. Soc.* **2005**, *127* (37), 12890–12899.
(21) Snaith, H. J.; Arias, A. C.; Morteani, A. C.; Silva, C.; Friend, R. H. *Nano Lett.* **2002**, *2* (12), 1353–1357.
(22) Rudzinski, W. E.; Lozano, L.; Walker, M. *J. Electrochem. Soc.* **1990**, *137* (10), 3132–3136.
(23) Wang, X. Z.; Shapiro, B.; Smela, E. *J. Phys. Chem. C* **2009**, *113* (1), 382–401.
(24) Hasanov, A.; Hasanoglu, S. *J. Math. Chem.* **2007**, *42* (4), 741–751.
(25) Otero, T. F.; Boyano, I. *J. Phys. Chem. B* **2003**, *107* (28), 6730–6738.
(26) Yamada, M.; Hagiwara, H.; Torigoe, H.; Matsumoto, N.; Kojima, M.; Dahan, F.; Tuchagues, J. P.; Re, N.; Iijima, S. *Chem. Eur. J.* **2006**, *12* (17), 4536–4549.
(27) Yasuda, H.; Lamaze, C. E.; Ikenberry, L. D. *Makromol. Chem.* **1968**, *118*, 19–35.
(28) Otero, T. F.; Grande, H.; Rodriguez, J. *Synth. Met.* **1996**, *83* (3), 205–208.
(29) Chang, Y. L.; Palacios, R. E.; Fan, F. R. F.; Bard, A. J.; Barbara, P. F. *J. Am. Chem. Soc.* **2008**, *130* (28), 8906–8907.
(30) Palacios, R. E.; Fan, F. R. F.; Grey, J. K.; Suk, J.; Bard, A. J.; Barbara, P. F. *Nature Mater.* **2007**, *6* (9), 680–685.
(31) Hou, Y.; Koeberg, M.; Bradley, D. D. C. *Synth. Met.* **2003**, *139* (3), 859–862.
(32) Richter, M. M.; Fan, F. R. F.; Klavetter, F.; Heeger, A. J.; Bard, A. J. *Chem. Phys. Lett.* **1994**, *226* (1−2), 115–120.
(33) Kim, J. I.; Shin, I. S.; Kim, H.; Lee, J. K. *J. Am. Chem. Soc.* **2005**, *127* (6), 1614–1615.
(34) Leland, J. K.; Powell, M. J. *J. Electrochem. Soc.* **1990**, *137* (10), 3127–3131.